Position Location and Trajectory Tracking for MUWT Based Kinematics Approach

Kun Yu[1,2], Guohua Xu[1] and Xiong Shen[1]
[1]College of Navy&Ship Science and Engineering, Huazhong University of Science and Technology, Wuhan, China
[2]China Ship Development and Design Center, Wuhan, China
Email: yukun198721@yahoo.com. hustxgh@yahoo.cn. buthold@sina.com

Abstract—**This paper describes an underwater 300m micro underwater work tool –MUWT(named huwt-3E, stands for three functions micro electric manipulator in China).The working principle and components of multi-sensors are introduced in detail. The pressure-compensated joint is compact designed and integrated of a micro permanent magnet (PM) brushless motor, a drive circuit, and an angular feedback potentiometer. The underwater control system is based network and consisted of three embedded system are used for servo control, task plan and target sensor respectively. Considering variable payload and uncertainty of model, a sliding mode control scheme is proposed to realize a MUWT with high precision. The control principle is based on the exponential approach law and a saturation function is introduced to solve the problem of chattering. A novel and simple self-adaptive regulation method is used to improve the velocity of approaching. Under the constant load and variable load, the simulation results of trajectory tracking show the effectiveness of the improved controller. The underwater test results verify the performance of controller in flow disturbance.**

Index Terms—**MUWT, Manipulator, Control Scheme, Trajectory Tracking, Position Location.**

I. INTRODUCTION

Robotic manipulators mounted on the Autonomous Underwater Vehicle (AUV) are extensively studied and called Underwater Vehicle-Manipulator Systems (UVMS)[1]. Motion of remotely operated UVMS is usually coordinated individually as a vehicle and a manipulator without using redundancy. However, for autonomous planning of trajectories corresponding to given task, redundant degrees of freedom (DOFs) of UVMS should be considered. Using redundancy resolution, motion of vehicle and manipulator can be coordinated simultaneously. In recent decades, the precise control of Manipulator mounted on autonomous underwater vehicle becomes a hot researching topic. The micro underwater work tools (UVMT) has the characters of nonlinear, coupled, time-varying and high dimension for the strong interactions between the dynamic of the vehicle and the manipulator, especially in the condition of the strong hydrodynamic forces[2],[3].

In underwater environment, the exact dynamic model of manipulator system is also difficultly established. In addition, variable payload including underwater flow effect on the underwater manipulator is the other difficulty. In this paper, some researches on the uncertainty in the system (variable payload, model uncertainty) are introduced. In order to deal with the uncertainty, sliding mode control (SMC) is applied in an electric underwater manipulator trajectory tracking control [4]-[7]. Sliding mode control (SMC) was proposed in twenty century fifties. For example, M.Belhocine applied SMC on a real manipulator arm which is SCARA robot. Giorgio Bartolini successfully applied SMC to an underwater grappler. The SMC system is claimed to have robust performances such as insensitivity to variations parameter and complete rejection of disturbances. Lots of job about SMC has been done[8],[9].

An electric manipulator with two degrees of freedom (DOF) which can be mounted on the autonomous underwater vehicle (AUV) is discussed in the paper. The main difficulty in controlling the manipulator is caused by non-linear dynamics of the system and the uncertainty in the system (variable payload, inertia, joint friction, etc.).There are lots of advanced algorithms are invited to deal with those problems. Lots of them are based on the model of the manipulator [9]-[13].

The paper is organized as follows: Implement of the whole system is present in Section II. Meanwhile, a SMC controller and some improvements is designed for 3-DOF underwater manipulator are described Section III. The position controller design is illustrated in Section IV. The experiment results and analysis in manipulator trajectory tracking control using SMC and PID are presented in Section V and Section VI. Finally, the conclusions are presented.

II. SYSTEM OVERVIEW

The underwater control system is based network and consisted of three embedded PC/104 computers which are used for servo control, task plan and vision respectively. Fig. 1 shows 300m underwater working system. The A/D board, D/A board are of PC104 bus standards. Vxworks OS is used in the three embedded PC/104 computers.

Manuscript received November 13, 2011; revised December 20, 2011; accepted January 17, 2012.
Corresponding author: Kun Yu.

doi:10.4304/jcp.8.4.1020-1026

Like a hard disk, a Compact Flash card is the external memory of the embedded PC/104 computers. User's application program and the system operation system are stored in the Compact Flash card. Three embedded PC/104 computers communicate through User Datagram Protocol (UDP) multicast communication. A supervisor PC with a virtual 3D GUI is fiber linked to underwater control system.

The sensor system includes an underwater camera and a unique ultra-sonic probe array. Vision program is running in Vxworks OS in the embedded PC104 computer which is cable linked with the camera. In ultra-sonic probe design, similar with Kleeman [4] who introduced multi-sonar system, we design a three ultra-sonic probe array .The advantage of the convex surface arrangement is that it can obtain a larger detectable angle, and detect both the distance and approximate location of the target. The detectable angle of single probe is 11°,the probe array can cover 30°. In each work period, every probe emits pulses and receives reflect wave once. The core unit communicates with the plan embedded computer via RS232C asynchronous serial communication. Its baud rate is 11520bps.

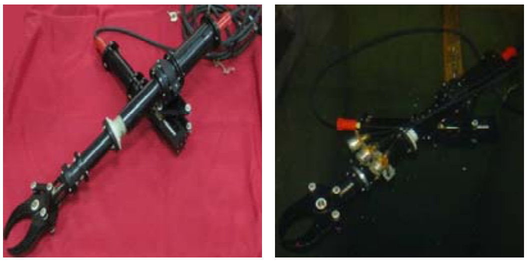

Figure 1. 300m manipulator in the air and under water.

Fig. 1 shows the 300m underwater working system.

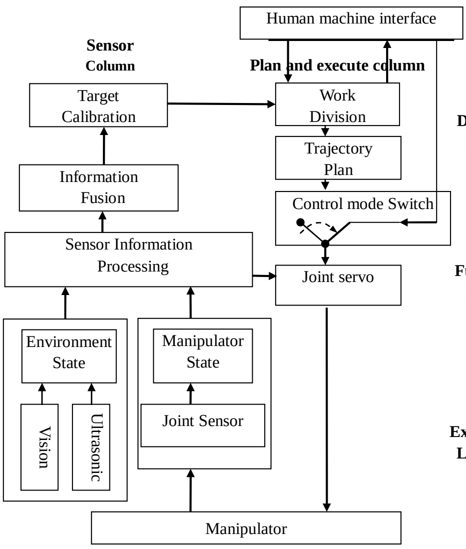

Figure 2. Structure of control system.

Fig. 2 shows the structure of control system. There are three layers: decision layer, function layer and execution layer. It has three modes (Remote, Automation and Autonomous control).In remote control mode, the operator controls the manipulator through keyboard. The control commend is in the low control level such as joint angle. The 3D graphic model displays the states of the manipulator and the target. In automation mode, when repetition task need to be done, after offline simulation, the planed trajectory data is saved and can be used more than once. In autonomous mode, the target information is obtained from vision and ultra sonic sensor. Once the target is in the range of sensors, the manipulator can work without operator's assistance.

III. Rule Velocity Controller Design

The manipulator introduced in this paper consists of a rotating joint and an extend/withdraw joint. Both of joints are driven by electric motors. The moving directions of two joints are vertical, so the coupling of the two joint can be ignored. It isn't necessary to use decoupling control methods usually used in serial linkage manipulators.

The moving directions of two joints are vertical, so the coupling of the two joint can be ignored. It isn't necessary to use decoupling control methods usually used in serial linkage manipulators. Because frictions between the surfaces of screws are sliding frictions, there are severe frictions in translational joint (joint 2). The translational joint will be studied clearly in this paper.

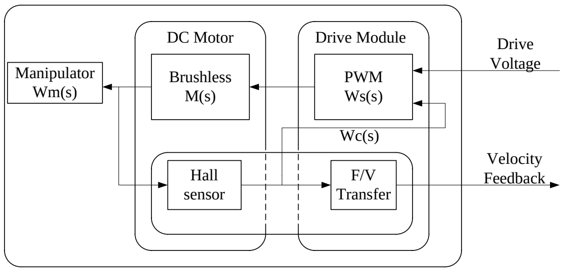

Figure 3. Feedback loop control model of manipulator.

The relationship parts in the manipulator system are shown in Fig. 3. The control system is comprised with three parts: drive module, DC motor and manipulator.

A. *Direct Current Brushless*

As sliding Mode Control doesn't need precise model, an ideal model of brushless DC motor is adopted without considering armature reaction and etc8 . The transfer function is

$$n(s)/U_{d0}(s) = 1/(C_e(T_m T_1 s^2 + T_m s + 1)) \quad (1)$$

Where $(n(s)U_{d0}(s))$ is Laplace transform of velocity.

TABLE I.
MOTOR PARAMETERS

Voltage	Power	Unload Velocity	Max Torque	Max current
24[V]	150[W]	<1000[RPM]	1[NM]	<6.5[A]

Armature loop electromagnetism time constant:

$$T_l = \frac{L}{R} = 0.8969 * 10^{-3} s \quad (2)$$

Anti electric potential parameter:

$$C=0.0298\ \text{V}\bullet\text{min/r} \tag{3}$$

Electric towage time constant:

$$T_m = GD^2R/(375C_eC_m) = 0.1123s \tag{4}$$

So

$$\begin{aligned}\frac{n(s)}{U_{d0}(s)} &= \frac{1/C_e}{T_mT_ls^2+T_ms+1}\\ &= \frac{33.557}{1.01*10^{-4}s^2+0.1123s+1}\end{aligned} \tag{5}$$

In two inertial systems:

$$M(s)=\frac{n(s)}{U_{d0}(s)}=\frac{33.557}{(9.07*10^{-4}s+1)(0.1114s+1)} \tag{6}$$

B. *Electric Drive Module*

1) Transfer Function of velocity Feedback Module: The velocity of motor is detected by a Hall sensor located in the motor. Through frequency and voltage (F/V) transfer electric circuit, the voltage of feedback signal of the sensor is with direct ratio to the impulse frequency generated by rotor revolving. There are Electric noises, so numeral filter is essential. Analysis the electric circuit, we take velocity feedback transfer module as one order inertial system. When motor works in linear regions, velocity feedback transfer function approximately is:

$$W_c\left(s\right)\approx k_p=5.546*10^{-3} \tag{7}$$

*2) Transfer Function of Pulse-Width Modulation (PWM):*Power amplifier: According to PWM mechanism, PWM power amplifier is a pure delay device. In usual electrical towage control systems, if the delay time is short, it can be approximately regarded as one order inertial system. Based on experiment, transfer function of Pulse-Width Modulation (PWM) power amplifier is:

$$W_s(s)\approx\frac{k_s}{T_ss+1}=\frac{5.8}{4.6*10^{-5}s+1} \tag{8}$$

C. *The Implements*

The extending length of manipulator is determined by the screw. The Hall sensor in motor generates pulse signals when the rotor revolves. While the motor revolves a circle, the arm extends or withdraws 4mm. so the number of pulse can stand for displacement of the arm.

$$Y=0.004*\int\frac{n}{60}dt(m) \tag{9}$$

n is velocity of motor(unit is radian per second).After Laplace transferring, written as:

$$W_m(s)=\frac{Y(s)}{N(s)}=\frac{k_g}{s}=\frac{1}{15000s} \tag{10}$$

D. Velocity Servo Controller

During the task of the deep sea manipulator, it will encounter lots of disturbing effect such as variable load, zero point shift and resistance rising in electric circuit causing by temperature rising and so on. In order to have anti disturbing character, velocity feedback is introduced in the servo control.

Proportion Integral controller is adopted and the transfer function is:

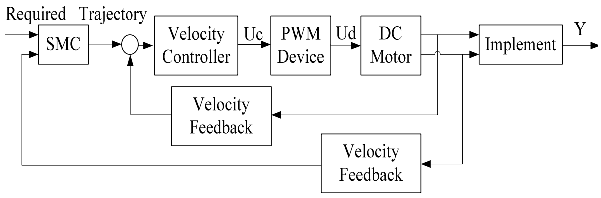

Figure 4. Double feedback loop control model.

$$w_{pi}(s)=\frac{k_{pi}(\tau_1s+1)}{\tau_1s}=\frac{k_{pi}(0.1114s+1)}{0.1114s} \tag{11}$$

As shown in Fig. 4, general system transfer function $D(s)$ is obtained after combining the transfer function of the several parts mentioned above.

$$\begin{aligned}D(s)&=\frac{w_{pj}(s)w(s)M(s)w_m(s)}{1+w_{pj}(s)w(s)M(s)w_m(s)}\\ &=\frac{2.772}{s(9.47*10^{-4}s^2+s+230.62)}\end{aligned} \tag{12}$$

IV. Position Controller Design

Sliding mode movements include reaching movement and sliding mode surface (sliding manifold) movement. System started from any initial states reaches to the switching surface." this period" is called approaching movement(s→0).According to the sliding mode control principle, it only guarantees that the sliding mode surface can be reached from any initial state within a finite time. There aren't any limits about the system trajectories. Different approaching method has different system dynamic quality. There are two key points in designing

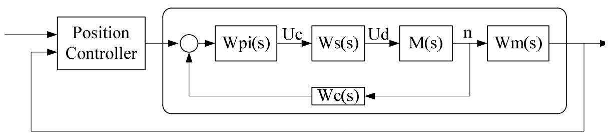

Figure 5. Double position feedback loop control model.

sliding mode control system: choosing switching function and solving the control law.

Fig. 5 shows the general system object structure.

A. Choosing Switching Function

The system in this paper is a single output (SISO) system whose switching function is input/single

$$\begin{aligned}s&=C^Tx\\ &=[C_1,C_2,\cdots C_{n-1},1][x_1,x_2,\cdots x_n]^T\\ &=C_1x_1+C_2x_2+\cdots C_{n-1}x_{n-1}+x_n\end{aligned} \tag{13}$$

Sliding manifold:

Choosing switching function is the problem how to solve the matrix C. We use the parameter of (13), into time at pole configuration method to solve first, change the system transfer domain form:

$$2.772u=9.47\times10^{-4}\dddot{y}+\ddot{y}+230.62\dot{y} \tag{14}$$

The states function is defined as:

$$\begin{cases} \dot{x} = Ax + Bu \\ y = Hx \end{cases} \tag{15}$$

$$A = \begin{bmatrix} 0 & 1 & 0 \\ 0 & 0 & 1 \\ 0 & -2.429\times10^5 & -1055.97 \end{bmatrix}, B = \begin{bmatrix} 0 \\ 0 \\ 2927.14 \end{bmatrix}$$

$$H = [1 \quad 0 \quad 0]$$

$$x = [x_0, x_1, x_2] = [y, \dot{y}, \ddot{y}]$$

So $\dot{Z} = A_{11}Z_1 + A_{12}Z_2$

Where $z_1 = [x_0, x_1]^T$, $z_2 = x_2$, $A_{11} = \begin{bmatrix} 0 & 1 \\ 0 & 0 \end{bmatrix}$, $A_{12} = \begin{bmatrix} 0 \\ 1 \end{bmatrix}$

$$\det(\lambda I - A_{11}) = \det\begin{bmatrix} \lambda & -1 \\ 0 & \lambda \end{bmatrix} = \lambda^2 \tag{16}$$

B. Exponential Approach Control Law

According to (14), we obtain

$$s = Ce = c_0e_0 + c_1e_1 + c_2e_2 \tag{17}$$

Choosing exponential Approach control law，

$$\dot{s} = -\varepsilon\,\mathrm{sgn}(s) - ks, (\varepsilon > 0) \tag{18}$$

Where $\dot{s} = c_0\dot{e}_0 + c_1\dot{e}_1 + c_2\dot{e}_2$

$$\dot{e}_2 = \frac{-\varepsilon\,\mathrm{sgn}(s) - ks - c_0\dot{e}_0 - c_1\dot{e}_1}{c_2} \tag{19}$$

Combining the two equations, control law can be obtained as:

$$\begin{aligned} u = {} & 3.146\times10^{-4}\left(\ddot{r}_d + \frac{\varepsilon\,\mathrm{sgn}(s) + ks + c_0\dot{e}_0 + c_1\dot{e}_1}{c_2}\right) \\ & + 0.3608(\ddot{r}_d - \dot{e}_1) + 83.196(\dot{r}_d - \dot{e}_0) \end{aligned} \tag{20}$$

Where $u = He + \varepsilon'\mathrm{sgn}(s) + k's + g$

Thus:

$$\begin{cases} H = \begin{bmatrix} 0 & \dfrac{3.14\times10^{-4}c_0}{c_2} - 83.2 & \dfrac{3.14\times10^{-4}c_1}{c_2} - 0.36 \end{bmatrix} \\ g = 3.14\times10^{-4}\dddot{r}_d + 0.36\ddot{r}_d + 83.2\dot{r}_d \\ \varepsilon' = \dfrac{3.14\times10^{-4}\varepsilon}{c_2} \\ k' = 3.14\times10^{-4}k / c_2 \end{cases} \tag{21}$$

C. Improvements of the Controller

If the switching function could work ideally, sliding mode control system designed above can gradually reach the original point through smooth movement. In actually, the sliding mode movement has chatter because of time the delay in the actual system. This is the main obstacle when applying SMC.

$$sat(s) = \begin{cases} 1 & s > \Delta \\ ks & |s| \le \Delta \\ -1 & s < \Delta \end{cases} \qquad k = \frac{1}{\Delta} \tag{22}$$

Here, continuous state feedback is used. $\mathrm{sgn}(s)$ in the slide mode can be replaced by saturate function $sat(s)$.

Where Δ is the thickness of boundary layer. In other words, outside the layer Δ， we choose control law as before. But we apply linear feedback control inside the layer Δ.

In sliding mode control based on exponential approaching law, the velocity of approaching is fast at the beginning and gradually reduces to zero while approaching to slide manifold. In order to accelerate the convergence, we hope that the velocity could be self-adjusted so that the error of tracking decreases to zero at me next sampling time, i.e.

$$s(k+1) = 0$$

According to the discrete equation

$$\dot{S} \approx [s(k+1) - s(k)]/T = -\varepsilon(k)\,\mathrm{sgn}(s(k) - ks(k)) \tag{23}$$

We obtain

$$\varepsilon(k) = \frac{1-kT}{T} * |s(k)| \tag{24}$$

$$u = He + \varepsilon' sat(s) + k's + g \tag{25}$$

Above all, we obtain the control law based on exponential approaching law:

Where:

$$H = \begin{bmatrix} 0 & \dfrac{0.0298c_0}{c_2} - 95.55 & \dfrac{0.0298c_1}{c_2} - 3.003 \end{bmatrix} \tag{26}$$

$$\varepsilon' = \frac{0.0298\varepsilon(k)}{c_2}, g = 0.0298\dddot{r}_d + 3.003\ddot{r}_d + 95.55\dot{r}_d \tag{27}$$

$$k' = 0.0298k / c_2, \varepsilon(k) = \frac{(1-kT)}{T} * |s(k)| \tag{28}$$

V. SIMULATION

A. Compare the Controller Improved with Unimproved

When me input trajectory $r(t) = 0.03\sin\omega t$ is given for the second joint of manipulator. In the experiment of unimproved method (k=70, ε=150), there are serious chattering; In other tests for the improved method, the chattering is reduced.

We can also decrease the ε to reduce the chattering. But in fact, we could not reduce discrete and switching character. Moreover, parameter k and ε need to be debugging so it isn't convenient.

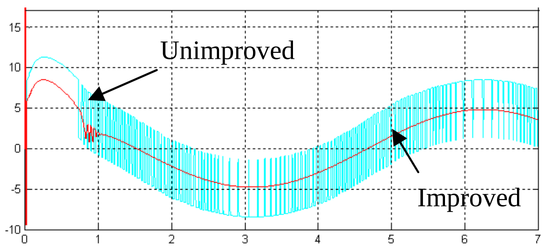

Figure 6. Controller's output before /after improved.

Through the output of the controller, we can find out the improvement before and after improved as Fig. 6.

B. Typical Tracking Simulation Result

Considering the system inertia, the actual velocity is smaller than the required velocity in time starts. After a short time, the effect of tracking is fine and the error of velocity becomes small.

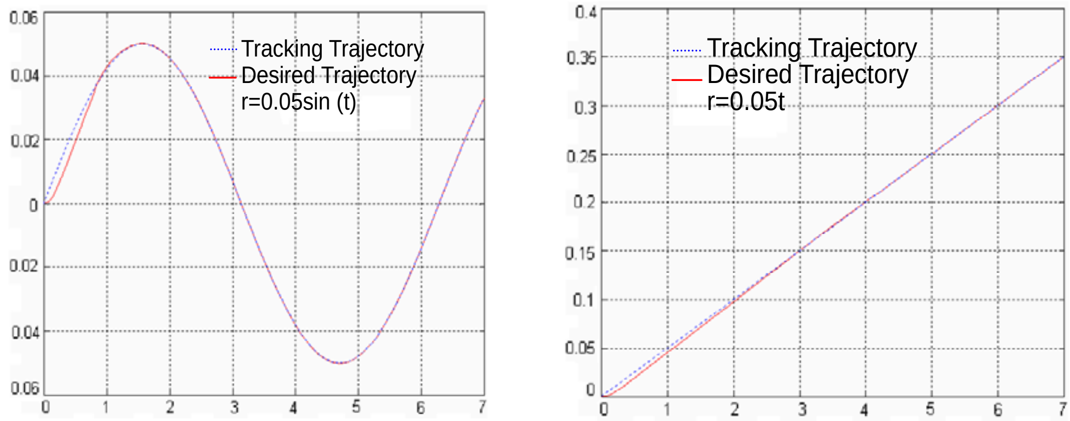

Figure 7. Trajectory curve of the end-effector.

Fig. 7 illustrates the effect.

1) Rated Load Test:

We suppose that rated burden is added to the system during time $[0,7]$s. The max-current that motor windings can be endured is the key parameter of the motor. With such limit, we choose $I_{dL}=0.7$ A as a load and the output of controller is showed in Fig. 8 (Desired tracking $r_{in}(t)=0.045\sin t$)

From the test we could tell that the tracking effect is

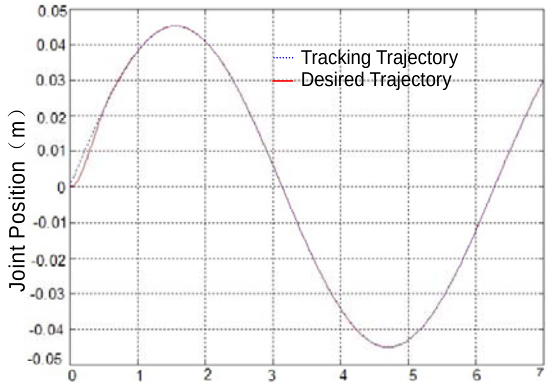

Figure 8. Trajectory curve of the end-effector

satisfying under the constant load.

2) Sudden Load Test:

In this test, we exert the sudden load at different period. Two periods are chosen: when velocity of manipulator is small and t large.

The loading current $I_{dL}(t)$ can be chosen in two circumstance.

$$I_{dL}(t)=\begin{cases}0.7A & t<t_1 \cup t>t_2\\ 4A & t\in[t_1,t_2]\end{cases} \tag{29}$$

Fig. 9 illustrates the effect.

VI. Controller And Result Analysis

The whole control system including a module "PC104" and "works". The structure of the hallow is based on a platform a real time operation system software system is shown as Fig. 10.

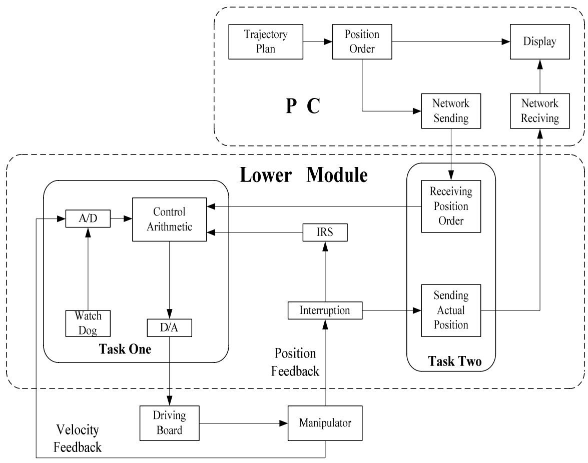

Figure 10. Structure of software system.

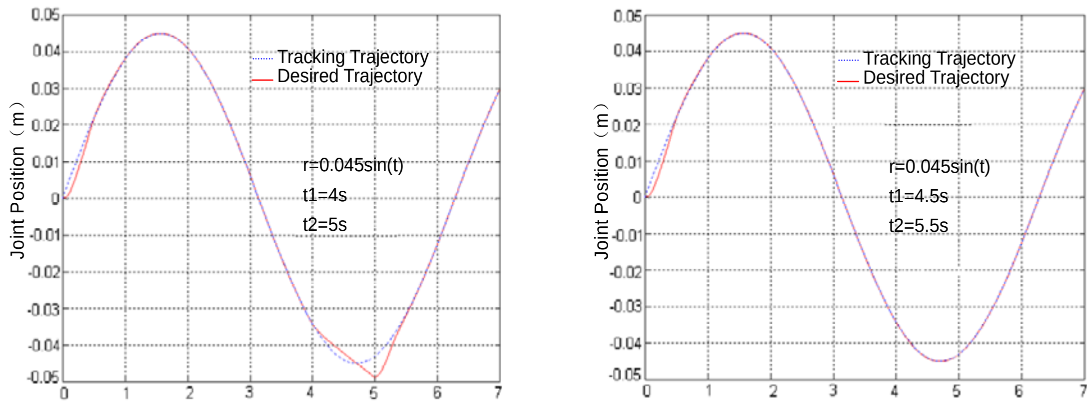

Figure 9. Two typical trajectory tracking curve in variable r.

The system consists of two parts-upper and lower: upper module is a PC with windows OS, and a friendly interface made by Microsoft Visual C++ 6. Through net sockets, the lower module receives the position orders sent from PC. Results given by software running on PC display both the planed trajectory and trajectory feedback.

A. Manipulator Tracking Experiment

In order to study the actual performance of the control method, trajectory tracking experiments were done. We mainly tested the joint 2 where severe sliding frictions existed.

1) Manipulator tracking without load: We give the desired trajectory(joint 2 $r_d = 30\sin(\pi t/10)$ mm.joint 1 $r_\theta = 0$),as Fig. 11 shows:

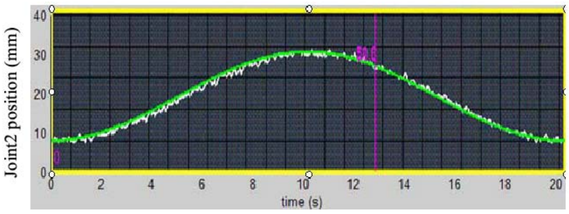

Figure 11. Manipulator tracking without load.

We found that: there are high frequency chatters near the desired trajectory. Although this chattering is disadvantage to high precision control, it benefits to overcome the frictions. Even though at low velocity, manipulator tracks well.

2) Manipulator tracking with sudden load: We give the desired trajectory (joint 2 $r_d = 75\sin(\pi t/10)$ mm.joint 1 $r_\theta = 0$ mm),as Fig. 12 shows:

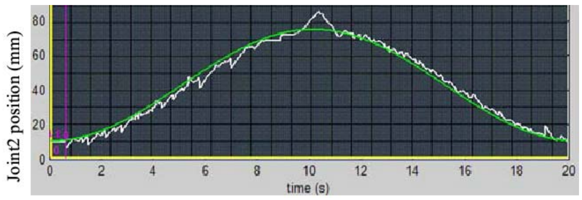

Figure 12. Manipulator tracking with sudden load.

Comparing with Fig. 11, we found that the tracking quality becomes worse. In the same frequency, when the amplitude is smaller, the tracking effect is better. If the amplitude A is small in equation $r(t) = A\sin(\omega t + \phi)$, the velocity (is derivative of $r(t)$)

So $\dot{r}(t) = A\cos(\omega t + \phi)$ isn't large in the same frequency ω .The range of velocity that can be changed is large. This is good for overcoming frictions. The sliding controller has robust character. The system added 9 Kg sudden load can also be converge.

B. Comparing with the PID Controller

In the comparing experiments, a PID controller is designed in the same experiment environment [9] .we choose one typical figure from lots of experiment results. The following results are obtained: In a special case Joint $r_d = 75\sin(\pi t/10)$ mm, joint 1 $r_\theta = 0$ mm), once the parameters of PID controller are optimal then the control effect is better than sliding mode controller. As Fig. 12 shows, the tracking quality is perfect at the beginning. However the PID controller could not perform well all the time. The parameters of PID controller should be adjusted to the situation. The system using PID controller could not overcome the friction moment existing in manipulator, so sometimes the manipulator can't be controlled. The sliding controller has robust character, even though there are sudden loads.

VII. Conclusions

Some improvements for a practical design of trajectory tracking control system based sliding mode control are proposed to deal with the chattering and approaching velocity for a MUWT. Results from simulation demonstrate that they have better advantages than traditional method and the controller is robust with respect to the un-exact model and also to payload variation. Even though we have considered various hydrodynamic effects and the modeling uncertainty in the simulations, hydrodynamic effects and the modeling uncertainties in practical situations might be more complicated. There are some improvements left to be done in future. For instance, the dynamic models of the motors and the thrusters also need to be included into the MUWT model in the future research. We shall take further experiment on AUVMS to verify the performance of the controller and improve the control algorithm. Except that, the target cylinder is static and has artificial feature. Autonomous grasp unstructured objects in more complex environment will be studied. The design of an underwater 300m electric manipulator is presented. And the dynamic models of the motors and the thrusters also need to be included into the MUWT model in the future research.

Acknowledgment

This work was funded by the China Nation Science and Technology Major Project (2011ZX05027-04), the China National 863 Program “deep-sea manipulator key technique” project (2006AA09Z203) and National Science Foundation of China (Grant No. 50909046 and No.51079061).

References

[1] G. Marani, S. K. Choi and J. Yuh, “Underwater autonomous manipulation for intervention missions AUVs,” Ocean Engineering, vol. 36, no. 1, pp. 15-23, Jan. 2009.

[2] Q. K. Liang, D. Zhang and Q. J. Song, “A potential 4-D fingertip force sensor for an underwater robot manipulator,” IEEE Journal of Oceanic Engineering, vol. 35, no. 3, pp. 574-583, Sep. 2010.

[3] G. Marani, S. K. Choi, “Underwater target localization,” IEEE Robotics & Automation Magazine, vol. 17, no. 1, pp. 64-70, Jan. 2010.

[4] L. Kleeman, R. Kuc, “Mobile robot sonar for target localization and classification,” The Int. Journal of Robotics Research, vol. 14, no. 4, pp. 295-318, Dec. 2005.

[5] D. G. Lowe, “Distinctive image features from scale-invariant key points,” International Journal of Computer Vision, vol. 60, no. 2, pp. 91-110, Mar. 2004.

[6] P. A. Azarbayejani, "Recursive estimation of motion, structure and focal length," IEEE Trans. on Pattern Analysis and Machine Intelligence, vol. 17, no. 6, pp. 562-575, Jun. 2005.
[7] B. Xu, S. Abe, N. Sakagami, and S. R. Pandian, "A Robust Nonlinear Controller for Underwater Vehicle-Manipulator Systems," in Proc. of the 2005 IEEE/ASME, Int. Conf. on Advanced Intelligent Mechatronics. Monterey, US, 2005, pp. 711-716.
[8] C.H. Santos, G. Bittencourt, and R. Guenther, "Motion Coordination for Underwater Vehicle-manipulator Systems using a Fuzzy Hybrid Strategy," in Proc. Of Int. Conf. on Intelligent Robots and Systems. Beijing, China, 2009, pp. 3018-3023.
[9] De Wit C. Canudas, Diaz O. Olguin and M. Perrier, "Nonlinear control of an underwater vehicle/manipulator with composite dynamics," IEEE Trans. on Control Systems Technology, vol. 8, no. 6, pp. 948-960, Jun. 2000.
[10] Y. S. Takashi, M. T. Sagara, "Digital type disturbance compensation control of a floating underwater robot with 2 link manipulator," Artifi. Life Robotics, vol. 13, no.1, pp.377-381, Jan. 2008.
[11] S. Sagara, M. Tamura, T. Yatoh and K. Shibuya, "Digital RAC for underwater vehicle-manipulator systems considering singular configuration," Artif Life Robotics, vol. 10, no.1, pp. 106-111, Jan. 2006.
[12] Joo H. Kim, J. Z. Yang and A. M. Karim, "A novel formulation for determining joint constraint," Multibody System Dynamics, vol. 10, no.1, pp. 427-451, Jan. 2008.
[13] De G. Novi, C. Melchiorri, J. C. García, "New approach for a reconfigurable autonomous underwater vehicle for Intervention," IEEE Aerospace and Electronic Systems Magazine, vol. 25, no. 11, pp. 32-36, Nov. 2010.

Kun Yu is currently a PhD in Huazhong University of Science and Technology, China. She received the master degree from HUST in 2008.

Currently she is working as a research assistant in the Automation Robotics, School of Navy and Ship Science and Engineering, China. Her research interests include data computer fusion, multi-computer control, Automation control of underwater vehicle.

Guohua Xu is currently a professor in huazhong University of Science and Technology, wuhan, China. He got the doctor degree from huazhong University of Science and Technology in 2000.

Professor Xu is working as Vice Dean in Mechanical Engineering, Key Laboratory of Education Ministry for Image Processing and Intelligent Control in China. His research areas include Multi-computer control, Information Fusion, Marine Engineering, Underwater robots, Automation Robotics,

Xiong Shen is currently a Ph.d in huazhong University of Science and Technology,wuhan,China.he recvied the master degree from huazhong University of Science and Technology in 2009.

Currently he is working as a research assistant in the Automation Robotics, Navy and Ship Science and Engineering, China.His research interests include Automation of Underwater vehicle, data integration,,computer security ,distribution computer, Automation contorol of Underwater vehicle .